LETTER

Carbon and alkalinity outwelling across the groundwater-creek-shelf continuum off Amazonian mangroves

Alex Cabral [ID],[1]* Thorsten Dittmar [ID],[2,3] Mitchell Call [ID],[4] Jan Scholten [ID],[5] Carlos E. de Rezende [ID],[6] Nils Asp [ID],[7] Martha Gledhill [ID],[8] Michael Seidel [ID],[2] Isaac R. Santos [ID][1,4]

[1]Department of Marine Sciences, University of Gothenburg, Gothenburg, Sweden; [2]Institute for Chemistry and Biology of the Marine Environment, University of Oldenburg, Oldenburg, Germany; [3]Helmholtz Institute for Functional Marine Biodiversity, University of Oldenburg, Oldenburg, Germany; [4]National Marine Science Centre, Southern Cross University, Coffs Harbour, Australia; [5]Institute of Geosciences, Christian Albrechts University, Kiel, Germany; [6]Aquatic Biogeochemistry Group, Universidade Estadual do Norte Fluminense Darcy Ribeiro, Campos dos Goytacazes, Brazil; [7]Institute for Coastal Studies, Federal University of Pará, Bragança, Brazil; [8]GEOMAR, Helmholtz Centre for Ocean Research Kiel, Kiel, Germany

Scientific Significance Statement

Carbon sequestration in mangroves is often estimated from their sediment storage capacity. However, lateral transport (outwelling) of dissolved carbon and alkalinity from intertidal wetlands can also drive long-term storage in the ocean. Here, we quantified outwelling rates across the groundwater-creek-shelf continuum of the world's largest continuous mangrove belt in the Amazon region. Dissolved inorganic carbon (DIC) fluxes exceeded dissolved organic carbon over all spatial scales. Since $90\% \pm 13\%$ of mangrove-derived DIC was bicarbonate, there is potential for long-term carbon storage offshore. Outwelling seems to exceed sediment burial as a carbon sequestration pathway in this and other mangrove-dominated coastlines.

Abstract

Lateral fluxes (i.e., outwelling) of dissolved organic (DOC) and inorganic (DIC) carbon and total alkalinity were estimated using radium isotopes at the groundwater, mangrove creek, and continental shelf scales in the Amazon region. Observations of salinity and radium isotopes in the creek indicated tidally driven groundwater exchange as the main source of carbon. Radium-derived transport rates indicate that mangrove carbon is exported out of the continental shelf on timescales of 22 ± 7 d. Bicarbonate was the main form ($82\% \pm 11\%$) of total dissolved carbon in all samples, followed by DOC ($13\% \pm 12\%$) and CO_2 ($5\% \pm 4\%$). DIC (18.7 ± 15.7 mmol m^{-2} d^{-1}) exceeded DOC (3.0 ± 4.1 mmol m^{-2} d^{-1}) outwelling at all spa-

---

tial scales. The interpretation of outwelling across the mangrove-ocean continuum is related to the spatial and temporal scales investigated. At all scales, outwelling represented a major coastal carbon pathway driving bicarbonate storage in the ocean.

Mangroves have one of the highest aerial carbon burial rates due to high primary production and complex root systems that allow organic matter deposition and long-term storage in the anoxic soil layers (Alongi 2020; Jennerjahn 2020). Part of the mangrove soil carbon might be released to the atmosphere after microbial decomposition and exported to ocean as particulate and dissolved matter (Bouillon et al. 2008; Volta et al. 2020). Outwelling is the lateral or horizontal transport of suspended and dissolved material at the land–ocean interface (Santos et al. 2021). Tidally driven groundwater exchange or tidal pumping is often the main pathway releasing carbon and alkalinity from mangrove sediments to coastal waters (Maher et al. 2018; Saderne et al. 2021). However, outwelling rates across the mangrove-ocean continuum and the related carbon storage in the ocean over the long term remain poorly quantified.

Methods to estimate outwelling include measuring geochemical tracers (e.g., radium and radon) over tidal cycles in mangrove creeks (Maher et al. 2013) and transects across the continental shelf (Sippo et al. 2019). Estimates of outwelling at the tidal creek scale do not capture carbon transformations by biogeochemical processes before potential storage in the ocean. In contrast, outwelling estimates at the shelf scale integrate carbon fluxes from multiple sources including rivers and mangroves (Dittmar et al. 2006). Radium isotopes can reveal coastal mixing, residence times, outwelling, and groundwater discharge in coastal regions (Moore 2000*b*; Dulaiova et al. 2006). However, there is lack of outwelling estimates over different spatial scales, making it difficult to fully constrain blue carbon budgets.

Here, radium-derived outwelling estimates were performed in the world's longest continuous belt of mangroves and on the continental shelf in the Amazon region. We compare total alkalinity (TA), dissolved organic carbon (DOC), and dissolved inorganic carbon (DIC) outwelling at multiple scales (groundwater, mangrove creek, and continental shelf), and discuss if outwelling can drive long-term carbon sequestration in the ocean.

Methods

Study sites

The study was conducted in the Furo do Meio mangrove creek, the Caeté Estuary and in the North Brazil continental shelf about 300 km southeast of the Amazon River mouth (Fig. 1). Furo do Meio is a 4.5 km long creek draining an intertidal catchment of 2.2 km^2 dominated by *Rhizophora mangle* (Dittmar et al. 2001). This site has well-developed mangroves with ~ 30 m high trees, a mature intertidal bank, and a monsoon-like climate with temperature of 28.6 ± 1.3°C

(Nobre et al. 2009). The creek receives no upstream freshwater inputs other than local precipitation, reaching 3300 mm during the wet season (December to May) to negligible amounts during the dry season (September to November) (Nobre et al. 2009) when mangrove creek sampling was performed.

The nearby Caeté River estuary receives freshwater discharge at ~ 50 m^3 s^{-1} from a 2061 km^2 watershed (Asp et al. 2018) with an estuary fringed by extensive mangroves wetlands. The tidal ranges are ~ 2.6 m in the neap tides and > 5 m in spring tides (Call et al. 2019). The Amazon continental shelf extends 330 km into the Atlantic. This region is a biogeochemical hotspot, receiving inputs from the world's longest continuous mangrove belt (542 km) and largest river basin (Dittmar et al. 2006; Hayashi et al. 2018). Earlier carbon cycle research in this area has quantified CO_2 and CH_4 emissions (Call et al. 2019), soil carbon burial (Kauffman et al. 2018; Matos et al. 2020), and DOC sources (Dittmar et al. 2001, 2006). Here, we focus on radium isotopes and inorganic carbon fluxes.

Sampling and analyses

We sampled groundwater ($n = 12$), the tidal creek ($n = 40$), estuary ($n = 21$), and the continental shelf ($n = 13$) to estimate fluxes at multiple scales (Fig. 1). The creek was sampled between 26 and 28 September 2017 during a neap tidal cycle and between 06 and 07 October 2017 during a spring tidal cycle. Water samples were collected hourly using a sample-rinsed polypropylene syringe and 0.7 μm Whatman GF/F filters. DIC and DOC were collected in precombusted 40 mL borosilicate vials containing 50–100 μL of saturated HgCl$_2$. TA was collected in 30 mL polypropylene vials (Mos et al. 2021). A calibrated Hydrolab DS5 logged temperature, salinity, and dissolved oxygen (DO) every minute. Depth and current velocity were logged at 1 min intervals using a Unidata Starflow (model 6526).

Surface-water samples for the Caeté estuary were collected on 10 October 2017 (Fig. 1c). Shelf samples were collected in two transects between 05 and 06 May 2018 during a GEOTRACES study (RV *Meteor cruise M147*, GApr11) (Fig. 1b). Shelf waters were sampled with Niskin bottles mounted on a CTD rosette at ~ 5 m depth and filtered with a peristaltic pump using a Causapure prefilter cartridge (1 μm, polypropylene, Infiltec) and a Causa-PES filter cartridge (0.1 μm, polyethersulfone, Infiltec). Radium samples were collected using a WASP-5 underwater pump at 2 m depth.

Groundwater was collected between 07 and 11 October 2017 at low tide from the mangrove forest. Holes were dug to ~ 0.5 m and purged before sampling with a peristaltic pump. Radium isotopes were sampled by filtering between 16 and
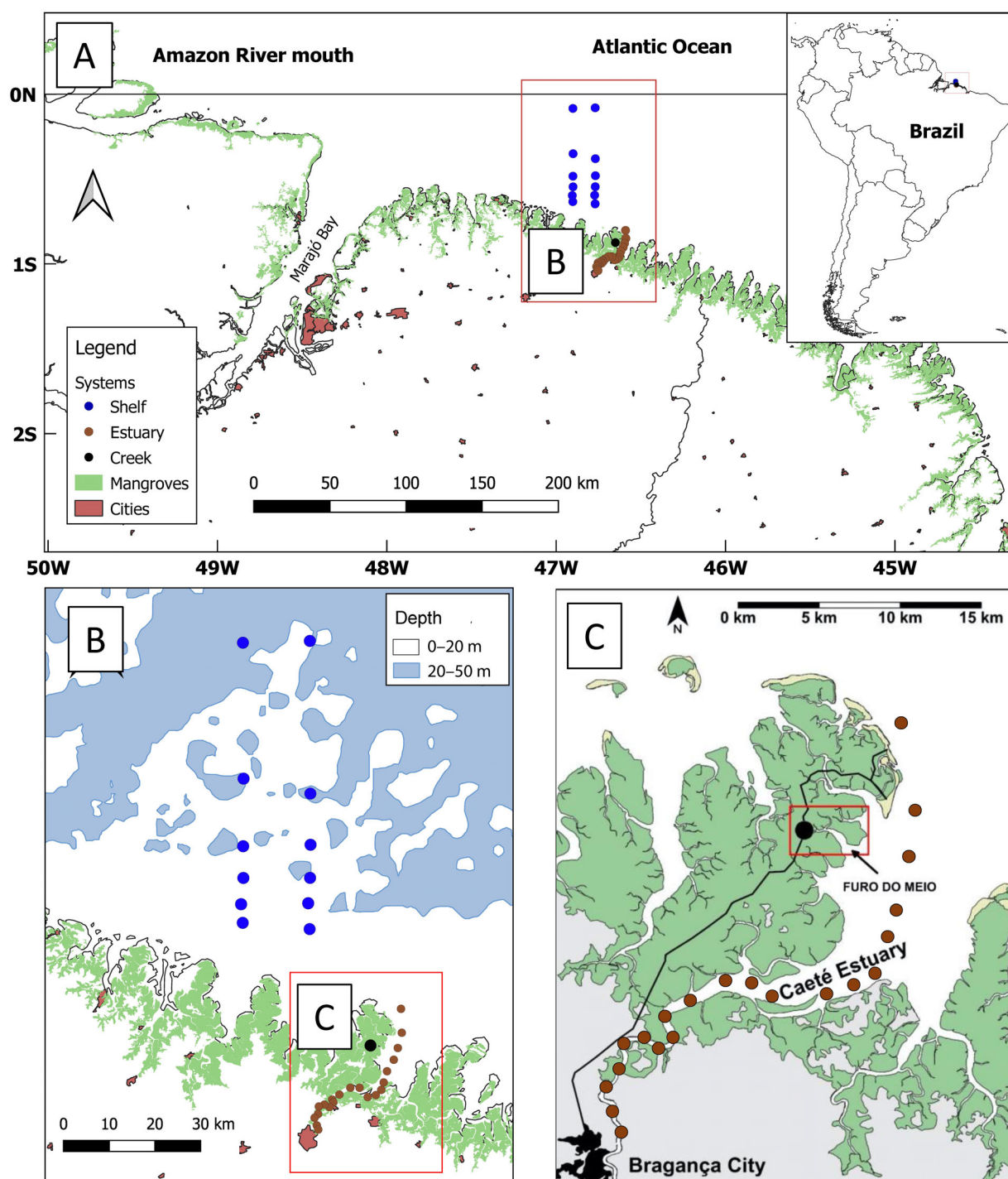
Fig 1. Study site (**a**) and sampling (**b** and **c**) locations at the groundwater-creek-estuary-shelf continuum in northern Brazil. Mangrove and urbanization cover were acquired from the Brazilian Institute of Environment and Natural Resources (IBAMA) and Brazilian Institute of Geography and Statistics (IBGE).

236 L of water through Mn fibers at < 1 L min^{-1}. The fibers were rinsed with radium-free water, partially dried, and placed in a Radium Delayed Coincidence Counter (RaDeCC) to measure ^{224}Ra and ^{223}Ra (Moore and Arnold 1996).

DOC samples were run through an OI Aurora 1030W or a Shimadzu TOC-VCPH instrument. DOC precision and trueness were tested against deep seawater reference material and low carbon water (provided by D. A. Hansell, University of

Miami) and both were < 5%. TA was measured using Gran titration with 0.01 mol L^{-1} HCl in a Metrohm Titrando (Mos et al. 2021). DIC was measured using a DIC analyzer (Apollo Scitech). Samples were calibrated using measurements of certified reference material from the Scripps Institution of Oceanography. HCO_3^- and CO_2 concentrations were calculated using CO2calc (Robbins et al. 2010) based on TA and DIC.

Estimating outwelling at different scales

Short-lived isotope (^{224}Ra and ^{223}Ra) time series in the tidal creek were used to calculate groundwater exchange during spring and neap tides using a mass balance (Gleeson et al. 2013) that considers tidal exchange, groundwater inputs, and decay. Water discharge ($m^3\ h^{-1}$) was calculated by the tidal prism variation in the creek (Maher et al. 2013). Tidal inputs (flood) and outputs (ebb) were estimated by multiplying the radium concentration (dpm m^{-3}) by discharge for each time step. These fluxes were integrated over complete tidal cycles during the neap and spring tides. The volume of groundwater leaving the creek over each tidal cycle ($m^3\ d^{-1}$) was estimated by dividing the net radium exports (dpm d^{-1}) by the average groundwater endmember concentration (dpm m^{-3}).

Concentrations in groundwater minus average concentrations in surface waters during high tide were assumed to represent the groundwater endmember after seawater recirculation in the sediments (Call et al. 2019; Santos et al. 2019). Outwelling at the mangrove creek scale was calculated by multiplying the water flow by carbon concentrations at each time step and integrating over complete tidal cycles (Sadat-Noori et al. 2015; Wadnerkar et al. 2021). Groundwater and creek outwelling were scaled for the mangrove intertidal area (2.2 km^2).

In order to estimate outwelling at the shelf scale, offshore eddy diffusivity mixing coefficients (K_h) were calculated using the slopes of the log-linear gradient in shelf radium isotope distributions (Moore 2000a, 2007). Carbon and TA outwelling across the shelf was calculated by multiplying their linear slopes by the average mixing coefficients (K_h) and the average depth of the mixed layer (~ 10 m) (Santos et al. 2009; Sippo et al. 2019). DIC and TA slopes were calculated using the excess concentration (ΔDIC and ΔTA) in relation to their conservative mixing (Liu et al. 2021) to correct for the effects of dilution (Supporting Information Fig. S1). A river sample was used as the freshwater endmember.

Radium ages were determined at two transects < 80 km offshore. This approach assumes that the shoreline is the only source of radium and that mixing and radioactive decay are the only sinks (Dulaiova and Burnett 2008). The relative differences of radium ages across the transects were used to estimate the offshore linear transport rate of radium (Peterson et al. 2008b). Fluxes of DOC, DIC, and TA from river were estimated by multiplying concentrations of freshwater samples (Fig. 1c) in the area upstream of mangroves by the discharge of the Caeté River (Brazilian Water Agency—Station Nova

Mocajuba). Fluxes and outwelling uncertainties were propagated for all systems (Harvard 2015).

Results

Mangrove groundwater

Mangrove groundwater salinity ranged from 26.2 to 39.1. DO (2.7 ± 3.2 mg L^{-1}) was often below saturation, reaching hypoxic levels (< 2.0 mg L^{-1}) in 40% of samples (Supporting Information Fig. S3). Groundwater had the highest concentrations of radium isotopes, carbon, and TA (Supporting Information Table S1, Figs. S2, S4). Groundwater exchange from the mangrove sediments to the creek oscillated from 1.5 ± 1.2 to 2.2 ± 2.0 cm d^{-1} using ^{223}Ra and ^{224}Ra, respectively, and 2.2 km^2 of intertidal mangrove area (Supporting Information Table S2). Groundwater fluxes of DOC, DIC, and TA were 4.8 ± 4.4, 18.2 ± 19.6, and 6.9 ± 11.3 mmol m^{-2} mangrove d^{-1}, respectively (Supporting Information Table S4).

Tidal creek

The creek depth ranged from 0.8 to 5.6 m and the tidal amplitude ranged from 2.1 to 4.7 m at neap and spring tides, respectively (Fig. 2). Creek salinity was higher at low tide (36.5 ± 0.5) than high tide (34.2 ± 0.6) due to evapotranspiration in the intertidal zone (Fig. 2). The tidally integrated water flow was 409 ± 372 $m^3\ d^{-1}$, which is equivalent to $0.6\% \pm 0.6\%$ of the tidal prism volume. Carbon, TA, and radium isotopes followed an inverse tidal trend in the creek (Fig. 2) with concentrations during low tide exceeding high tide values by a factor of 1.6–3.4. Outwelling of DOC, DIC, and TA at the creek scale were 0.3 ± 10.0, 20.0 ± 13.7, and 15.2 ± 8.3 mmol m^{-2} mangrove d^{-1}, respectively.

Caeté River estuary

During the spatial survey in the estuary, salinity fluctuated between 1.1 (most upstream sample) and 36.9 in the mouth of the estuary (Supporting Information Fig. S4). Radium isotopes, DOC, ΔTA, and ΔDIC showed the highest concentrations in the section of the estuary where most of the mangrove forests are located (Supporting Information Figs. S4, S6). The river fluxes of DOC, DIC, and TA were 0.07 ± 0.01, 0.63 ± 0.03, and 0.55 ± 0.06 mmol m^{-2} catchment d^{-1}, respectively.

Continental shelf

Radium activities (^{224}Ra and ^{223}Ra) in the continental shelf decreased in the offshore direction (Fig. 3) implying a nearshore radium source. DOC concentrations also significantly ($p < 0.05$) decreased toward the open ocean, whereas TA and DIC increased (Fig. 3). Excess of DIC and TA, however, decreased toward offshore (Supporting Information Fig. S1d). Radium ages increased from 5.7 d nearshore to 14.3 d in the most offshore sample (83 km), resulting in an integrated cross-shore transport of 9.0 ± 3.3 cm s^{-1} or 7.8 ± 2.9 km d^{-1}.
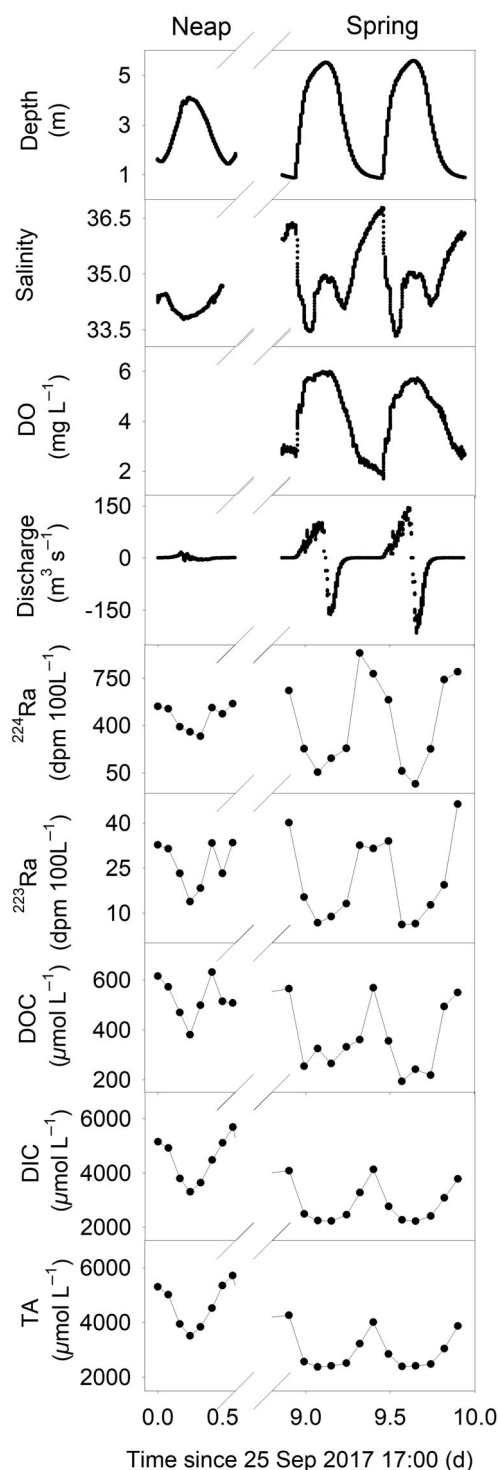
Fig 2. Time series in the mangrove creek during the neap (15 h) spring (25 h) tide cycles. Depth, salinity, and DO were measured with 1 min frequency. Radium isotopes, DIC, DOC, and TA were sampled with 2 h frequency. Positive discharge indicates flood tide while negative discharges indicate ebb flows.

DOC, DIC, and TA outwelling at shelf scale was $7.8 \pm 3.2 \times 10^5$, $9.9 \pm 3.3 \times 10^6$, and $1.2 \pm 0.9 \times 10^6$ mmol m^{-1} shoreline d^{-1}, respectively (Supporting Information Table S3).

Normalizing fluxes against areas is challenging because we do not know the exact spatial scale represented by radium measurements. If we assume 542 km of mangrove shoreline (Hayashi et al. 2018), outwelling of DOC, DIC, and TA at the shelf scale would convert to 1.4 ± 0.6, 18.2 ± 6.1, and 2.3 ± 1.7 mmol m^2 shelf d^{-1}, respectively. While these cross-shelf fluxes are likely explained by a combination of river and mangrove sources, we cannot separate their relative contribution at the shelf scale because shelf and mangrove observations were performed at different seasons.

Discussion

Radium isotopes

Carbon outwelling in mangroves is triggered by the exchange of intertidal groundwater enriched in carbon through crab burrows (Taillardat et al. 2018; Taniguchi et al. 2019). The daily variability of depth, salinity, and radium isotopes (Fig. 2) indicates that groundwater exchange in the mangrove creek is driven by tidal pumping. Similar patterns were observed for nutrients, CO_2, CH_4, and ^{222}Rn in the same tidal creek, implying a common source (Dittmar and Lara 2001; Call et al. 2019). The groundwater exchange rates derived from ^{224}Ra (2.2 ± 2.0 cm d^{-1}) and ^{223}Ra (1.5 ± 1.2 cm d^{-1}) were comparable to other mangroves worldwide ranging between 0.3 and 84 cm d^{-1} (Chen et al. 2018). Differences among systems occur due to variable tidal ranges, sediment composition, and climatic conditions (Taillardat et al. 2018).

At the continental shelf, both ^{224}Ra and ^{223}Ra showed a clear log-linear pattern (Fig. 3), suggesting that conservative mixing and decay rather than advection drives radium distribution as observed in the South Atlantic Bight (Moore 2000*a*) and off mangroves in Australia (Sippo et al. 2019). The radium-derived transport rates in the shelf (9.0 ± 3.3 cm s^{-1}) were higher than other nearshore systems, such the Yellow Sea (3.3–4.7 cm s^{-1}, Peterson et al. 2008*a*) likely due to large tidal ranges in North Brazil. Considering the continental shelf width (~ 200 km) in the Amazon mangrove belt region and radium transport rates, it would take 22.3 ± 7.2 d for mangrove carbon to cross the shelf and reach the open ocean, where it can be stored over long timescales.

Carbon speciation

In spite of an early focus on DOC (Dittmar et al. 2006; Rezende et al. 2007; Kristensen et al. 2008), DIC was the dominant form of carbon in all compartments. Mangroves retain high organic content in sediments. Part of this organic matter is mineralized via aerobic and anaerobic processes which consume particulate organic carbon (POC) and DOC and produce DIC (Taillardat et al. 2018). DIC and DOC were significantly correlated ($r^2 = 0.65$, $p < 0.001$), especially in the creek samples, indicating that both carbon species have a similar source (Supporting Information Fig. S5). Overall, radium-derived DIC outwelling was 4-65 times higher than DOC, suggesting that
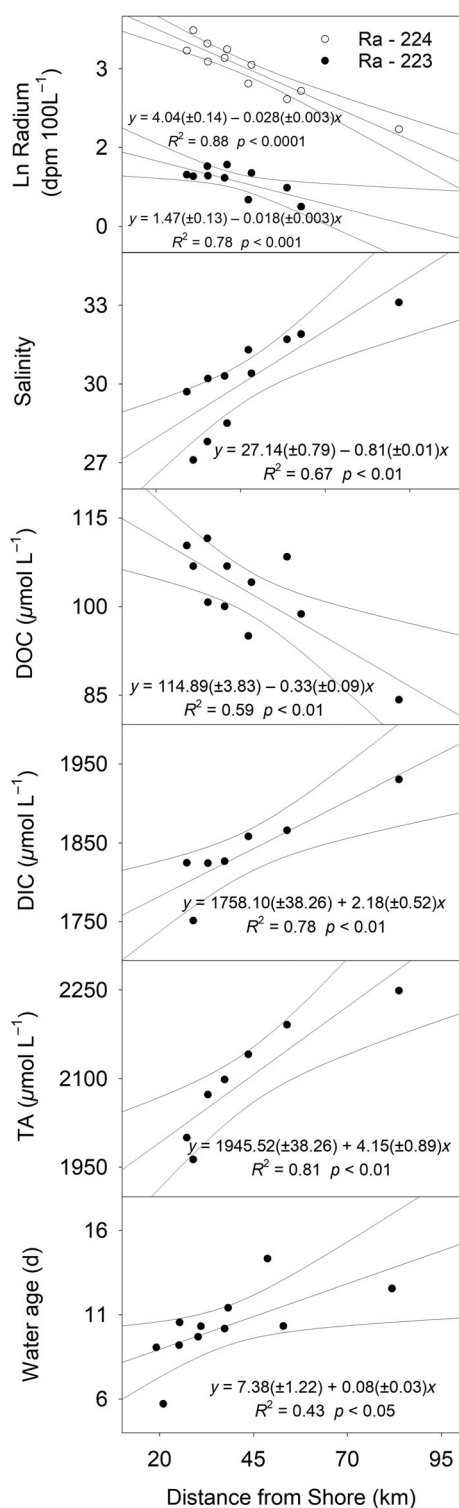
Fig 3. Offshore coastal transects of radium isotopes, salinity, TA, and DIC and DOC in seawater sampled in May 2018. Water ages were calculated from ^{224}Ra : ^{223}Ra ratios. ΔTA and ΔDIC were used to estimate shelf scale outwelling as shown in Fig S1.

inorganic carbon is the main form exported to the coastal ocean as expected for mangrove-dominated coasts (Alongi 2020; Santos et al. 2021).

The relationship between DIC and TA provides insights into the pathways of organic matter mineralization (Bouillon et al. 2007). The DIC : TA slopes were calculated by the deviation of DIC (ΔDIC) and total alkalinity (ΔTA) concentrations from the conservative mixing (Supporting Information Fig. S4) to avoid the effects of simple dilution across samples with different salinities (Liu et al. 2021). The slopes imply that the production of DIC and TA can be a result of different biogeochemical reactions, especially at the estuary and shelf scales due to sources other than mangroves. Sulfate reduction seems to represent the main organic carbon mineralization pathway within the mangrove (groundwater and tidal creek samples) as observed in other mangrove systems (Sippo et al. 2016; Twilley et al. 2019; Reithmaier et al. 2020). However, other processes, such as calcium carbonate dissolution, might represent an important source of alkalinity in mangroves and on the shelf (Macreadie et al. 2017; Volta et al. 2020; Saderne et al. 2021).

Most studies assume that carbon sequestration in mangroves occurs primarily via sediment burial. However, this underestimates carbon storage in the ocean following outwelling of bicarbonate or refractory DOC (Maher et al. 2018; Santos et al. 2019). Bicarbonate accounted for 82% ± 11% of the total dissolved carbon species, exceeding DOC (13% ± 12%) and dissolved CO_2 (5% ± 4%) at all scales (Fig. 4b). Alkalinity, mostly as bicarbonate, has a residence time of 100–1000 ka, allowing long-term storage in the ocean (Renforth and Henderson 2017).

### Carbon and alkalinity outwelling across different spatial scales

Estimating outwelling is challenging due to multiple physical and biogeochemical processes across the groundwater-mangrove-shelf continuum. Biogeochemical processes modifying carbon speciation as well as hydrological and oceanographic factors influence exports to the ocean (Gillis et al. 2017; Santos et al. 2021). Carbon and alkalinity outwelling varied across different spatial scales (Fig. 5). The highest outwelling fluxes were found at the groundwater and creek scales, within the range observed in mangroves worldwide (Alongi 2020). Since there is no freshwater input to the tidal creek, groundwater exchange was the major driver of dissolved carbon and alkalinity outwelling.

Studies quantifying carbon outwelling at cross-shore or continental shelf are scarce. Here, continental shelf outwelling rates were similar to those found at the mangrove scale, especially for DIC (Fig. 5), even though fieldwork occurred in different periods. Offshore sampling occurred during the wet season when rivers are a source of carbon to the shelf, whereas sampling in the creek was performed during the dry season when tidal pumping within mangroves is a major source of carbon (Call et al. 2019).

Using the average discharge for the Caeté river during the wet season (~ 80 m^3 d^{-1}), we found that DIC and TA fluxes are still higher in the tidal creek than in the river (Supporting Information Table S4). However, when extrapolating for the
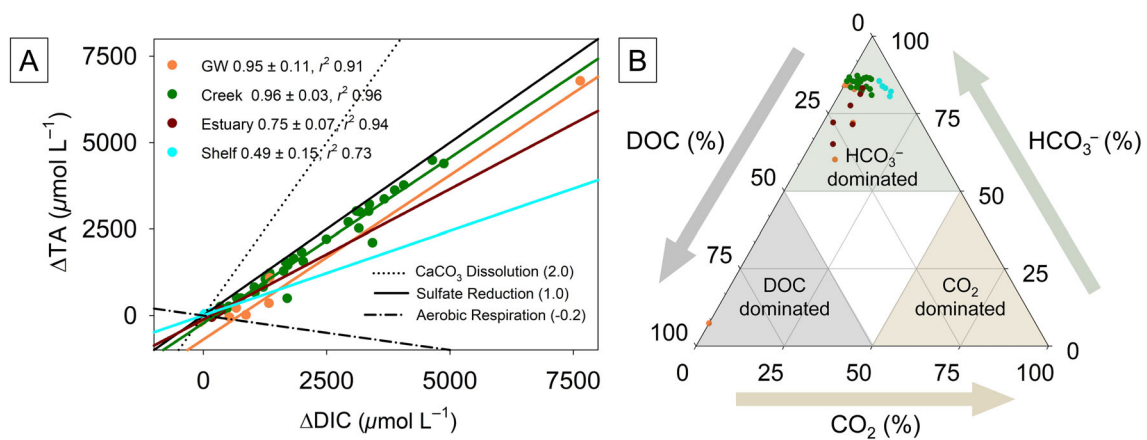
Fig 4. (**a**) Linear regressions between ΔTA and ΔDIC concentrations derived from their conservative mixing (Supporting Information Fig. S4). Only significant ($p < 0.05$) regressions (r^2) are shown. The biogeochemical processes slopes (parenthesis) are derived from Redfield C : N : P stoichiometry (106 : 16 : 1) (Bouillon et al. 2007; Krumins et al. 2013). The broader C : N : P ratios found in mangrove soil worldwide (282 : 9 : 1 to 2923 : 117 : 1) might modify the typical DIC : TA slopes (Scharler et al. 2015; Rovai et al. 2018). (**b**) Relative contribution of DOC, CO_2, and bicarbonate (HCO_3^-) in the mangrove-shelf continuum.
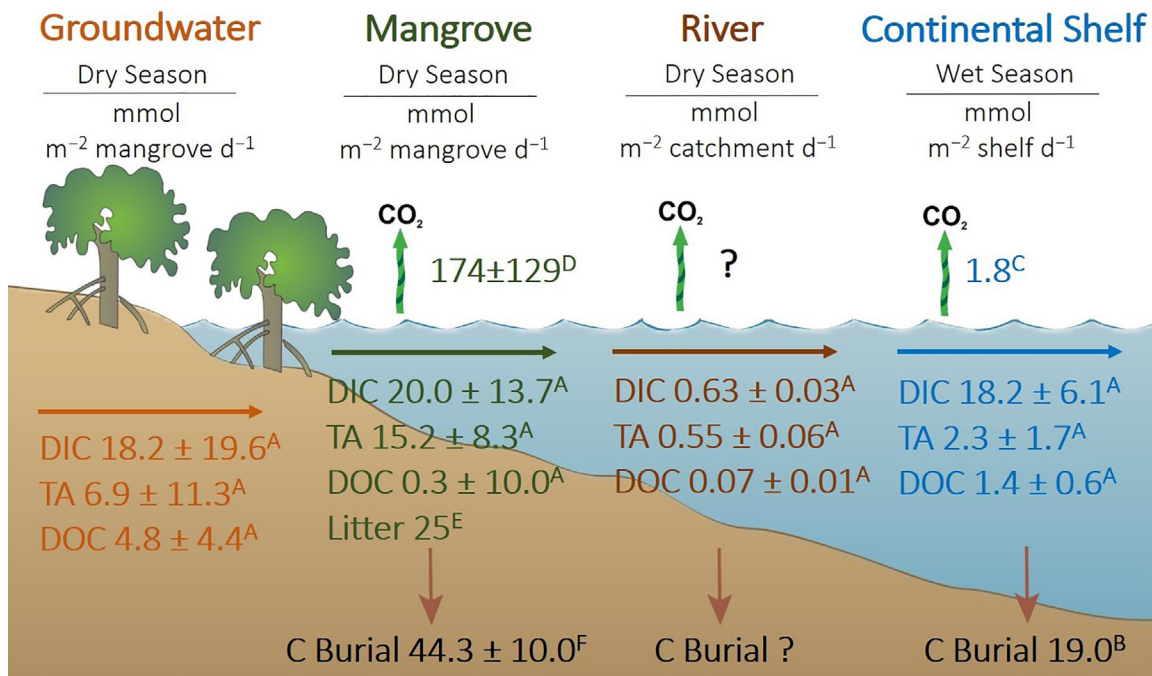
Fig 5. Conceptual model summarizing carbon (DOC and DIC) and TA fluxes, CO_2 emissions, and C sediment burial rates in the Amazonian groundwater-mangrove-shelf continuum. Superscript letters provide references for data based on our study (A); (B) Aller et al. (1996); (C) Lefèvre et al. (2017); (D) Call et al. (2019); (E) Dittmar and Lara (2001); (F) Matos et al. (2020). Additional outwelling rates in mmol d^{-1} and mmol m^{-1} shoreline d^{-1} can be found in the Supporting Information Tables S3, S4.

Amazon mangrove belt (mmol d^{-1}), carbon fluxes were 2–8 times higher in rivers than mangroves during the wet season, indicating that both temporal and spatial scales should be considered when comparing outwelling rates.

Previous studies in the same shelf area during the dry season estimated DOC outwelling of 33.3 mmol m^{-2} mangrove d^{-1}

(Dittmar et al. 2006). Although the shelf scale integrates outwelling from multiples sources, this area includes ~ 70% of Brazil's mangroves that play an important role delivering carbon southeast of the Amazon River (Dittmar et al. 2001). Carbon outwelling in the mangrove tidal creek was 13-50 times higher than the Caeté River during the dry season (Fig. 5).

Extrapolating these results to the Amazon mangrove belt and river watershed area (Supporting Information Table S4), mangrove outwelling rates (mmol d^{-1}) were 11–92 times higher than river fluxes in the dry season, showing that mangroves are the main source of carbon and alkalinity to the regional continental shelf during this period.

Total dissolved carbon plus litter outwelling was comparable to sediment burial rates (Fig. 5) estimated for nearby mangroves (Matos et al. 2020). At the shelf scale, total dissolved carbon outwelling exceeded burial rates (Aller et al. 1996) and CO_2 fluxes seem to represent a minor fraction (4.2%) of the carbon budget. While these comparisons are constrained by limited sampling, they highlight that overlooking outwelling followed by bicarbonate storage in the ocean may underestimate the carbon sequestration capacity of mangroves.

Carbon outwelling is usually estimated in one single compartment, that is, mangrove creek (Dittmar and Lara 2001; Taillardat et al. 2018) or continental shelf (Dittmar et al. 2006; Sippo et al. 2019). There is limited outwelling data across different scales, especially in mangrove-rich regions of South America and Africa (Santos et al. 2021). Future studies investigating multiple scales and vertical gradients are needed to provide additional insight into drivers of outwelling and decrease uncertainties of global estimates. Carbon isotopes can also reveal the relative contribution of different sources organic matter (Taillardat et al. 2018; Volta et al. 2020; Kwon et al. 2021). Combining radioactive and stable isotopes tracers will help to build complete carbon budgets for this region and elsewhere.

References

Aller, R. C., N. E. Blair, Q. Xia, and P. D. Rude. 1996. Remineralization rates, recycling, and storage of carbon in Amazon shelf sediments. Cont. Shelf Res. **16**: 753–786. doi:10.1016/0278-4343(95)00046-1

Alongi, D. M. 2020. Carbon balance in salt marsh and mangrove ecosystems: A global synthesis. J. Mar. Sci. Eng. **8**: 1–21. doi:10.3390/jmse8100767

Asp, N. E., and others. 2018. Sediment dynamics of a tropical tide-dominated estuary: Turbidity maximum, mangroves and the role of the Amazon River sediment load. Estuar. Coast. Shelf Sci. **214**: 10–24. doi:10.1016/j.ecss.2018.09.004

Bouillon, S., F. Dehairs, B. Velimirov, G. Abril, and A. V. Borges. 2007. Dynamics of organic and inorganic carbon across contiguous mangrove and seagrass systems (Gazi Bay, Kenya). J. Geophys. Res. Biogeosci. **112**: 1–14. doi:10.1029/2006JG000325

Bouillon, S., and others. 2008. Mangrove production and carbon sinks: A revision of global budget estimates. Global Biogeochem. Cycles **22**: 1–12. doi:10.1029/2007GB003052

Call, M., I. R. Santos, T. Dittmar, C. E. de Rezende, N. E. Asp, and D. T. Maher. 2019. High pore-water derived CO_2 and CH_4 emissions from a macro-tidal mangrove creek in the Amazon region. Geochim. Cosmochim. Acta **247**: 106–120. doi:10.1016/j.gca.2018.12.029

Chen, X., F. Zhang, Y. Lao, X. Wang, J. Du, and I. R. Santos. 2018. Submarine groundwater discharge-derived carbon fluxes in mangroves: An important component of blue carbon budgets? J. Geophys. Res. Oceans **123**: 6962–6979. doi:10.1029/2018JC014448

Dittmar, T., and R. J. Lara. 2001. Driving forces behind nutrient and organic matter dynamics in a mangrove tidal creek in North Brazil. Estuar. Coast. Shelf Sci. **52**: 249–259. doi:10.1006/ecss.2000.0743

Dittmar, T., R. J. Lara, and G. Kattner. 2001. River or mangrove? Tracing major organic matter sources in tropical Brazilian coastal waters. Mar. Chem. **73**: 253–271. doi:10.1016/S0304-4203(00)00110-9

Dittmar, T., N. Hertkorn, G. Kattner, and R. J. Lara. 2006. Mangroves, a major source of dissolved organic carbon to the oceans. Global Biogeochem. Cycles **20**: 1–7. doi:10.1029/2005GB002570

Dulaiova, H., W. C. Burnett, G. Wattayakorn, and P. Sojisuporn. 2006. Are groundwater inputs into river-dominated areas important? The Chao Phraya River - Gulf of Thailand. Limnol. Oceanogr. **51**: 2232–2247. doi:10.4319/lo.2006.51.5.2232

Dulaiova, H., and W. C. Burnett. 2008. Evaluation of the flushing rates of Apalachicola Bay, Florida via natural geochemical tracers. Mar. Chem. **109**: 395–408. doi:10.1016/j.marchem.2007.09.001

Gillis, L. G., F. E. Belshe, A. D. Ziegler, and T. J. Bouma. 2017. Driving forces of organic carbon spatial distribution in the tropical seascape. J. Sea Res. **120**: 35–40. doi:10.1016/j.seares.2016.12.006

Gleeson, J., I. R. Santos, D. T. Maher, and L. Golsby-Smith. 2013. Groundwater-surface water exchange in a mangrove tidal creek: Evidence from natural geochemical tracers and implications for nutrient budgets. Mar. Chem. **156**: 27–37. doi:10.1016/j.marchem.2013.02.001

Harvard (2007). A Summary of Error Propagation. Cambridge, MA: Harvard University Press.

Hayashi, S. N., P. W. M. Souza-Filho, W. R. Nascimento, and M. E. B. Fernandes. 2018. The effect of anthropogenic drivers on spatial patterns of mangrove land use on the Amazon coast. PLoS One **14**: 1–20. doi:10.1371/journal.pone.0217754

Jennerjahn, T. C. 2020. Relevance and magnitude of "Blue Carbon" storage in mangrove sediments: Carbon accumulation rates vs. stocks, sources vs. sinks. Estuar. Coast. Shelf Sci. **247**: 107027. doi:10.1016/j.ecss.2020.107027

Kauffman, J. B., A. F. Bernardino, T. O. Ferreira, L. R. Giovannoni, L. E. O. de Gomes, D. J. Romero, L. C. Z. Jimenez, and F. Ruiz. 2018. Carbon stocks of mangroves and salt marshes of the Amazon region, Brazil. Biol. Lett. **14**: 20180208. doi:10.1098/rsbl.2018.0208

Kristensen, E., S. Bouillon, T. Dittmar, and C. Marchand. 2008. Organic carbon dynamics in mangrove ecosystems: A review. Aquat. Bot. **89**: 201–219. doi:10.1016/j.aquabot.2007.12.005

Krumins, V., M. Gehlen, S. Arndt, P. Van Cappellen, and P. Regnier. 2013. Dissolved inorganic carbon and alkalinity fluxes from coastal marine sediments: Model estimates for different shelf environments and sensitivity to global change. Biogeosciences **10**: 371–398. doi:10.5194/bg-10-371-2013

Kwon, E. Y., T. DeVries, E. D. Galbraith, J. Hwang, G. Kim, and A. Timmermann. 2021. Stable carbon isotopes suggest large terrestrial carbon inputs to the Global Ocean. Global Biogeochem. Cycles **35**: 1–25. doi:10.1029/2020GB006684

Lefèvre, N., and others. 2017. A source of CO_2 to the atmosphere throughout the year in the Maranhense continental shelf ($2°30'S$, Brazil). Cont. Shelf Res. **141**: 38–50. doi:10.1016/j.csr.2017.05.004

Liu, Y., J. J. Jiao, W. Liang, I. R. Santos, X. Kuang, and C. E. Robinson. 2021. Inorganic carbon and alkalinity biogeochemistry and fluxes in an intertidal beach aquifer: Implications for ocean acidification. J. Hydrol. **595**: 126036. doi:10.1016/j.jhydrol.2021.126036

Macreadie, P. I., O. Serrano, D. T. Maher, C. M. Duarte, and J. Beardall. 2017. Addressing calcium carbonate cycling in blue carbon accounting. Limnol. Oceanogr.: Lett. **2**: 195–201. doi:10.1002/lol2.10052

Maher, D. T., I. R. Santos, L. Golsby-Smith, J. Gleeson, and B. D. Eyre. 2013. Groundwater-derived dissolved inorganic and organic carbon exports from a mangrove tidal creek: The missing mangrove carbon sink? Limnol. Oceanogr. **58**: 475–488. doi:10.4319/lo.2013.58.2.0475

Maher, D. T., M. Call, I. R. Santos, and C. J. Sanders. 2018. Beyond burial: Lateral exchange is a significant atmospheric carbon sink in mangrove forests. Biol. Lett. **14**: 20180200. doi:10.1098/rsbl.2018.0200

Matos, C. R. L., J. F. Berrêdo, W. Machado, C. J. Sanders, E. Metzger, and M. C. L. Cohen. 2020. Carbon and nutrient accumulation in tropical mangrove creeks, Amazon region. Mar. Geol. **429**: 106317. doi:10.1016/j.margeo.2020.106317

Moore, W. S. 2000*a*. Determining coastal mixing rates using radium isotopes. Cont. Shelf Res. **20**: 1993–2007. doi:10.1016/S0278-4343(00)00054-6

Moore, W. S. 2000*b*. Ages of continental shelf waters determined from ^{223}Ra and ^{224}Ra. J. Geophys. Res. Oceans **105**: 22117–22122. doi:10.1029/1999JC000289

Moore, W. S. 2007. Seasonal distribution and flux of radium isotopes on the southeastern U.S. continental shelf. J. Geophys. Res. Oceans **112**: 1–16. doi:10.1029/2007JC004199

Moore, W. S., and R. Arnold. 1996. Measurement of ^{223}Ra and ^{224}Ra in coastal waters using a delayed coincidence counter. J. Geophys. Res. Oceans **101**: 1321–1329. doi:10.1029/95JC03139

Mos, B., C. Holloway, B. P. Kelaher, I. R. Santos, and S. A. Dworjanyn. 2021. Alkalinity of diverse water samples can be altered by mercury preservation and borosilicate vial storage. Sci. Rep. **11**: 9961. doi:10.1038/s41598-021-89110-w

Nobre, C. A., G. O. Obregón, J. A. Marengo, R. Fu, and G. Poveda. 2013. Characteristics of Amazonian climate: Main Features. *In Amazonia and Global Change* (eds M. Keller, M. Bustamante, J. Gash and P. Silva Dias). doi:10.1029/2009GM000903

Peterson, R. N., W. C. Burnett, M. Taniguchi, J. Chen, I. R. Santos, and T. Ishitobi. 2008*a*. Radon and radium isotope assessment of submarine groundwater discharge in the Yellow River delta, China. J. Geophys. Res. Oceans **113**: C09021. doi:10.1029/2008JC004776

Peterson, R. N., W. C. Burnett, M. Taniguchi, J. Chen, I. R. Santos, and S. Misra. 2008*b*. Determination of transport rates in the Yellow River-Bohai Sea mixing zone via natural geochemical tracers. Cont. Shelf Res. **28**: 2700–2707. doi:10.1016/j.csr.2008.09.002

Reithmaier, G., D. T. Ho, S. G. Johnston, and D. T. Maher. 2020. Mangroves as a source of greenhouse gases to the atmosphere and alkalinity and dissolved carbon to the coastal ocean: A case study from the Everglades National Park, Florida. J. Geophys. Res. Biogeosci. **125**: 1–16. doi:10.1029/2020JG005812

Renforth, P., and G. Henderson. 2017. Assessing ocean alkalinity for carbon sequestration. Rev. Geophys. **55**: 636–674. doi:10.1002/2016RG000533

Rezende, C. E., L. D. Lacerda, A. R. C. Ovalle, and L. F. F. Silva. 2007. Dial organic carbon fluctuations in a mangrove tidal creek in Sepetiba Bay, Southeast Brazil. Braz. J. Biol. **67**: 673–680. doi:10.1590/S1519-69842007000400012

Robbins, L., M. E. Hansen, J. Kleypas, and S. C. Meylan. 2010. CO2calc - a user-friendly seawater carbon calculator for Windows, Max OS X, and iOS (iPhone): U.S. Geological Survey Open-File Report 2010–1280, 17 p.

Rovai, A. S., and others. 2018. Global controls on carbon storage in mangrove soils. Nat. Clim. Chang. **8**: 534–538. doi:10.1038/s41558-018-0162-5

Sadat-Noori, M., I. R. Santos, C. J. Sanders, L. M. Sanders, and D. T. Maher. 2015. Groundwater discharge into an estuary using spatially distributed radon time series and radium isotopes. J. Hydrol. **528**: 703–719. doi:10.1016/j.jhydrol.2015.06.056

Saderne, V., M. Fusi, T. Thomson, A. Dunne, F. Mahmud, F. Roth, S. Carvalho, and C. M. Duarte. 2021. Total alkalinity production in a mangrove ecosystem reveals an overlooked Blue Carbon component. Limnol. Oceanogr.: Lett. **6**: 61–67. doi:10.1002/lol2.10170

Santos, I. R., W. C. Burnett, T. Dittmar, I. G. N. A. Suryaputra, and J. Chanton. 2009. Tidal pumping drives nutrient and dissolved organic matter dynamics in a Gulf of Mexico subterranean estuary. Geochim. Cosmochim. Acta **73**: 1325–1339. doi:10.1016/j.gca.2008.11.029

Santos, I. R., D. T. Maher, R. Larkin, J. R. Webb, and C. J. Sanders. 2019. Carbon outwelling and outgassing vs. burial in an estuarine tidal creek surrounded by mangrove and saltmarsh wetlands. Limnol. Oceanogr. **64**: 996–1013. doi: 10.1002/lno.11090

Santos, I. R., and others. 2021. The renaissance of Odum's outwelling hypothesis in "Blue Carbon" science. Estuar. Coast. Shelf Sci. **255**: 107361. doi:10.1016/j.ecss.2021. 107361

Scharler, U. M., and others. 2015. Variable nutrient stoichiometry (carbon:nitrogen:phosphorus) across trophic levels determines community and ecosystem properties in an oligotrophic mangrove system. Oecologia **179**: 863–876. doi: 10.1007/s00442-015-3379-2

Sippo, J. Z., D. T. Maher, D. R. Tait, C. Holloway, and I. R. Santos. 2016. Are mangrove drivers or buffers of coastal acidification? Global Biogeochem. Cycles **30**: 753–766. doi: 10.1002/2015GB005324

Sippo, J. Z., D. T. Maher, K. G. Schulz, C. J. Sanders, A. McMahon, J. Tucker, and I. R. Santos. 2019. Carbon outwelling across the shelf following a massive mangrove dieback in Australia: Insights from radium isotopes. Geochim. Cosmochim. Acta **253**: 142–158. doi:10.1016/j.gca.2019. 03.003

Taillardat, P., A. D. Ziegler, D. A. Friess, D. Widory, V. Truong Van, F. David, N. Thành-Nho, and C. Marchand. 2018. Carbon dynamics and inconstant porewater input in a mangrove tidal creek over contrasting seasons and tidal amplitudes. Geochim. Cosmochim. Acta **237**: 32–48. doi: 10.1016/j.gca.2018.06.012

Taniguchi, M., and others. 2019. Submarine groundwater discharge: Updates on its measurement techniques, geophysical drivers, magnitudes, and effects. Front. Environ. Sci. **7**: 1–26. doi:10.3389/fenvs.2019.00141

Twilley, R. R., V. H. Rivera-Monroy, A. S. Rovai, E. Castañeda-Moya, and S. Davis. 2019, *Mangrove biogeochemistry at local to global scales using ecogeomorphic approaches*. Elsevier B.V.

Volta, C., D. T. Ho, D. T. Maher, R. Wanninkhof, G. Friederich, C. Del Castillo, and H. Dulai. 2020. Seasonal variations in dissolved carbon inventory and fluxes in a mangrove-dominated estuary. Global Biogeochem. Cycles **34**: 1–27. doi:10.1029/2019GB006515

Wadnerkar, P. D., and others. 2021. Contrasting radium-derived groundwater exchange and nutrient lateral fluxes in a natural mangrove versus an artificial canal. Estuaries Coast. **44**: 123–136. doi:10.1007/s12237-020-00778-1